

## Design and Development of A Digital Soil Temperature Monitoring System Based on The Internet of Things at North Sumatra Climatological Station

Royston Manurung<sup>1,2</sup>, Tulus Ikhsan Nasution<sup>1\*</sup>, Syahrul Humaidi<sup>1</sup>, Immanuel Jhonson A. Saragih<sup>3</sup>, Khindi Aufa Hibatullah<sup>4</sup>, Marhaposon Situmorang<sup>1</sup>, Yahya Darmawan<sup>5</sup>

\*Corresponding author email : [ikhsan\\_05@yahoo.com](mailto:ikhsan_05@yahoo.com)

- <sup>1</sup> Department of Physics, Faculty of Mathematics and Natural Sciences – University of North Sumatra, Jl. Dr. T. Mansur No.9, Padang Bulan, Kec. Medan Baru, Kota Medan, Sumatera Utara, Indonesia. Postal code: 20222
- <sup>2</sup> BMKG – North Sumatra Climatological Station, Jl. Meteorologi Raya No.17, Tembung, Kec. Percut Sei Tuan, Kabupaten Deli Serdang, Sumatera Utara, Indonesia. Postal code: 20371
- <sup>3</sup> BMKG – Kualanamu Meteorological Station, Jl. Tengku Heran Pasar V Kebun Kelapa, Kec. Beringin, Kab. Deli Serdang, Sumatera Utara, Indonesia. Postal code: 20552
- <sup>4</sup> BMKG – Center for Meteorology, Climatology and Geophysics Region I (BBMKG Wilayah I), Jl. Ngumban Surbakti No.15, Sempakata, Kec. Medan Selayang, Kota Medan, Sumatera Utara, Indonesia. Postal code: 20131
- <sup>5</sup> BMKG – School of Meteorology, Climatology, and Geophysics (STMKG), Jl. Perhubungan I No.5, Pd. Betung, Kec. Pd. Aren, Kota Tangerang Selatan, Banten, Indonesia. Postal code: 15221

Received: December 14, 2023

Accepted: December 28, 2023

Published: December 28, 2023

Copyright © 2023 by author(s) and Scientific Research Publishing Inc.

Open Access



### Abstract

Soil temperature is a crucial parameter in monitoring and understanding climate and soil ecosystems. It plays a vital role in various environmental aspects, including agriculture, ecology, and geoscience. Monitoring soil temperature is necessary for planning and managing agriculture and natural resources. Currently, temporal observations of soil temperature by BMKG are limited, conducted only at 07:55, 13:55, and 18:55 local time. This limitation makes it difficult to perform detailed soil temperature analysis. This research was conducted to design a digital soil temperature monitoring device accessible via the internet. Seven DS18B20 sensors were used at depths of 0 cm, 2 cm, 5 cm, 10 cm, 20 cm, 50 cm, and 100 cm, combined with an ESP8266 module using the Arduino system. The implementation of this design resulted in a real-time soil temperature monitoring system with data updates every 10 seconds. The observed data are displayed on a 20x4 LCD and sent to the cloud, making them accessible on the webpage <http://monitoringsuhutanah.my.id>. Calibration results indicate that the DS18B20 sensors used in this study provide accurate and consistent temperature measurements, with an average correction range of (-0.20) to 0.24, thus suitable for operational use. Field tests show that the digital data are accurate and correspond (linearly correlate) with conventional data. This is based on a correlation value of 0.7, while the RMSE values range from 0.5 to 2.18 and the bias ranges from (-0.69) to 0.08.

**Keywords:** Soil Temperature, DS18B20 Sensors, ESP8622, Arduino

### 1. Introduction

Soil is one of the most important and complex natural resources on Earth. It plays a key role in supporting human life and ecosystems, as it performs a number of crucial ecological functions (Brady et al., 2008; Rose, 2004). Soil serves as the growth medium for plants and provides habitat for various organisms.

Soil temperature is a measure of the heat or warmth of the soil at a certain depth below the Earth's surface (Campbell & Norman, 1998). It is a significant parameter in soil science, agriculture, and various other applications, as soil temperature affects numerous biological, physical, and chemical

processes within soil ecosystems (Campbell & Norman, 1998; Hatfield & Prueger, 2015; Salam, 2020). Soil temperature is measured using soil thermometers or implanted in the soil.

Observational data on soil temperature play a vital role in agroclimatic monitoring, particularly in the context of agriculture and natural resource management. This data provides valuable insights into soil conditions that can impact plant growth, agricultural productivity, and the sustainability of farming ecosystems. With a good understanding of soil temperature, farmers can manage irrigation more efficiently, avoiding over-irrigation or under-irrigation. Soil temperature observation data are not only crucial in supporting sustainable agriculture but also in mitigating the impacts of climate change on food production and ecosystem sustainability. Therefore, accurate and continuous monitoring of soil temperature is a valuable asset in efforts to maintain food security and a healthy environment.

The Meteorology, Climatology, and Geophysics Agency (BMKG) holds significant responsibility in weather and climate monitoring in Indonesia, including soil temperature observation. Currently, BMKG still uses standard thermometers implanted in the soil at certain depths for temperature measurement (shown in Figure 1). This conventional method of observation has limitations, requiring substantial human resources and time, and is prone to human error in thermometer readings. The limited frequency of observations means that this conventional soil temperature monitoring system cannot provide real-time data. Therefore, there is a need to transform the soil temperature observation system from conventional tools to digital ones based on the Internet of Things (IoT).

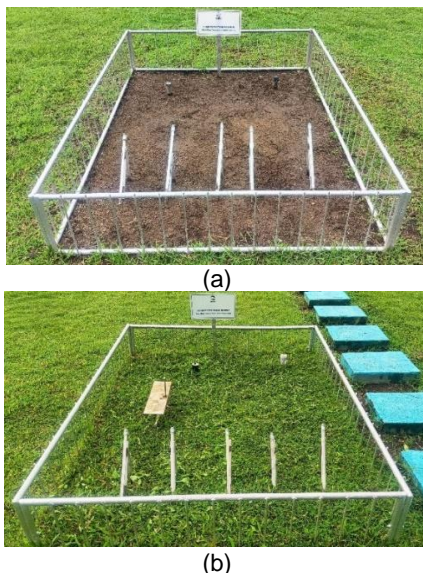


**Figure 1.** The bare soil thermometer (a) and grass-covered soil thermometer (b) existing at the North Sumatra Climatological Station

The transformation of the soil temperature observation system is a critical step in more accurate, efficient, and responsive weather and climate monitoring, particularly in light of global climate change. The digital system employs modern sensors and devices that can provide more precise and timely

measurements. This allows for the acquisition of better and more reliable weather data. Digital tools enable real-time weather monitoring, thus enhancing the monitoring of soil temperature changes.

This research was conducted to design a soil temperature observation system based on the Internet of Things (IoT) at the North Sumatra Climatological Station using DS18B20 sensors, a Real Time Clock (RTC) module, and NodeMCU ESP8266. In addition to being displayed on an LCD, the digital observational data is also transmitted to the cloud for storage and can be accessed on a webpage via the internet. To measure the performance of the device, calibration and field tests were conducted in this study. This research is expected to produce a reliable and beneficial IoT-based soil temperature observation system for the North Sumatra Climatological Station and a broader range of soil temperature data users.

## 2. Method

### 2.1 Block Diagram

The block diagram in Figure 2 represents the overall design of the system to be developed in this study. The block diagram consists of three parts: Input, Process, and Output. The input to this system comes from three main components. Firstly, the DS18B20 temperature sensor is used to measure soil temperature at various depths. This sensor provides the necessary temperature data for monitoring environmental conditions. Secondly, the Real-Time Clock (RTC) module is responsible for providing accurate time information for the system. This is crucial for recording the time of soil temperature measurements conducted by the DS18B20 sensor. Lastly, the power supply provides operational power to the entire system.

The main process in this block diagram is carried out by the NodeMCU ESP8266. NodeMCU acts as the brain of the system, tasked with collecting data from the DS18B20 temperature sensor and the RTC module. Subsequently, NodeMCU manages this data and controls the 20x4 LCD display to show relevant information such as soil temperature and measurement time. Additionally, the NodeMCU ESP8266 has a very important additional function. It acts as a bridge between the system and the internet, enabling the data generated by the sensors and the RTC module to be uploaded to a server or website via an internet connection. This opens up opportunities for remote monitoring and data storage in a format accessible to users via a website.

In this way, this block diagram represents a well-integrated soil temperature observation system, from the measurement of temperature by sensors to the display of data on the LCD and data storage and access via the internet. This provides a comprehensive solution for Internet of Things (IoT)-based soil temperature monitoring.

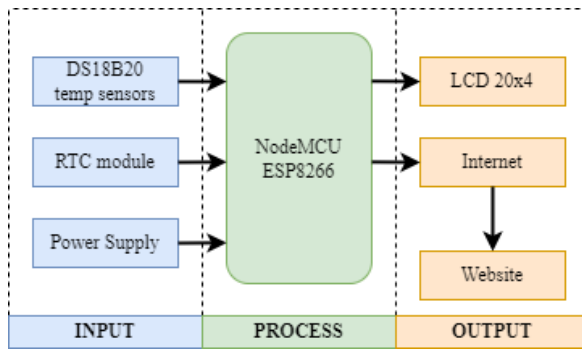


Figure 2. Block diagram used in this research

## 2.2 System Design

The system design encompasses both the schematic and the conceptual design of the system. The system design schematic is a diagram of the assembled electronic components, arranged according to their function, serving as a reference in the creation of the soil temperature measuring device.

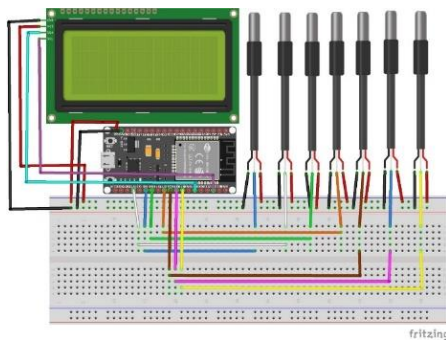


Figure 3. Schematic system design

Figure 3 presents the schematic of the system design used in the study. The conceptual design addresses the physical appearance of the device. Figure 4 shows the conceptual design of the system, which comprises several components, including the DS18B20, Real-Time Clock (RTC), ESP8266, 20x4 LCD, and a breadboard power supply. In this study, the DS18B20 sensor is designed to be waterproof.

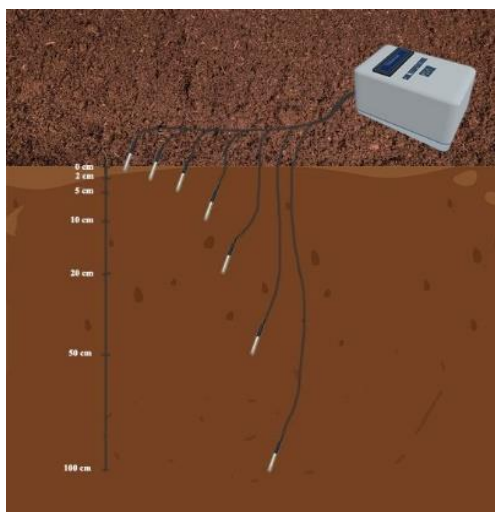


Figure 4. Conceptual system design

## 2.3 System Validation

System validation is conducted to ensure that the data generated by the Internet of Things (IoT)-based digital soil temperature observation system designed in this study has adequate accuracy and consistency. The validation stages in this research include the calibration of the DS18B20 temperature sensor and the verification of digital data against conventional observational data.

### a) Calibration of DS18B20 sensors

Calibration is carried out to ensure that the DS18B20 sensor used can accurately measure temperature. The calibration process is conducted at the Calibration Laboratory - Center for Meteorology, Climatology, and Geophysics Region I. According to the World Meteorological Organization (WMO) in the document 'Guide to Instruments and Methods of Observation' (WMO-No. 8), it is stated that the calibration range is  $-30^{\circ}\text{C}$  to  $+40^{\circ}\text{C}$  with a correction tolerance of  $\pm 0.2^{\circ}\text{C}$ . Based on this, calibration in this study is performed with four readings at each set point of  $15^{\circ}\text{C}$ ,  $25^{\circ}\text{C}$ , and  $35^{\circ}\text{C}$ .

### b) Verification of digital data against conventional data

Verification is carried out by comparing the data generated by the digital system with available conventional observational data. The comparison is done statistically by calculating the Mean Absolute Error (MAE), Mean Squared Error (MSE), Root Mean Square Error (RMSE), R-squared, Mean Absolute Percentage Error (MAPE), Bias, and Correlation Coefficient. The following are the statistical equations used below:

$$MAE = \frac{\sum(X_{obs} - X_{sensor})}{n} \quad (1)$$

$$MSE = \frac{\sum(X_{obs} - X_{sensor})^2}{n} \quad (2)$$

$$RMSE = \sqrt{MSE} = \sqrt{\frac{[\sum(X_{obs} - X_{sensor})]^2}{n}} \quad (3)$$

$$R^2 = 1 - \frac{\sum(X_{obs} - X_{sensor})^2}{\sum(X_{obs} - X_{rata2})^2} \quad (4)$$

$$MAPE = \frac{1}{n} \sum \left| \frac{X_{obs} - X_{sensor}}{X_{obs}} \right| \times 100\% \quad (5)$$

$$Bias = \frac{1}{n} \sum (X_{obs} - X_{sensor}) \quad (6)$$

$$r = \frac{n(\sum X_{obs} X_{sensor}) - [(\sum X_{obs})(\sum X_{sensor})]}{\sqrt{[n \sum X_{obs}^2 - (\sum X_{obs})^2][n \sum X_{sensor}^2 - (\sum X_{sensor})^2]}} \quad (7)$$

The verification was carried out in accordance with the availability of conventional observational data conducted at the North Sumatra Climatological Station, as shown in Table 1. Digital observational data at 08.00 local time (LT) and 14.00 LT at depths of 0 cm, 2 cm, 5 cm, 10 cm, and 20 cm are compared against conventional observational data at 07.55 LT and 13.55 LT. Meanwhile, digital data at 18.00 LT are compared with conventional data at 17.55 LT.

**Table 1.** Scheme for verifying digital data against conventional data

Sensor/Thermometer Depth	Observation Time (LT)					
	Conventional Data			Digital Data		
	07.55	13.55	17.55	08.00	14.00	18.00
0 cm	✓	✓	✓	✓	✓	✓
2 cm	✓	✓	✓	✓	✓	✓
5cm	✓	✓	✓	✓	✓	✓
10 cm	✓	✓	✓	✓	✓	✓
20 cm	✓	✓	✓	✓	✓	✓
50 cm	X	X	✓	X	X	✓
100 cm	X	X	✓	X	X	✓

### 3. Result and Discussion

#### 3.1 System Implementation

System implementation refers to the final output of the designed device. In this study, the system implementation is divided into two parts: hardware implementation and software implementation. The core of this system is the application of the integrated DS18B20 temperature sensor, strategically placed at various stratified depths: surface (0 cm), shallow (2 cm, 5 cm), medium (10 cm, 20 cm), and deep (50 cm, 100 cm). This system is programmed to automatically collect data at scheduled intervals, reducing the need for manual intervention and increasing operational efficiency. The collected data are then transmitted in real-time through the Internet of Things, a connected network that facilitates data exchange.

##### a) Hardware implementation

The DS18B20 sensors are installed in seven holes at varying depths of 0 cm, 2 cm, 5 cm, 10 cm, 20 cm, 50 cm, and 100 cm. The installation of the DS18B20 sensors is carried out following the instructions provided in the sensor datasheet. The DS18B20 has pins that must be connected to the NodeMCU ESP8266 microcontroller. Programming of the NodeMCU ESP32 microcontroller is done using the Arduino programming language.

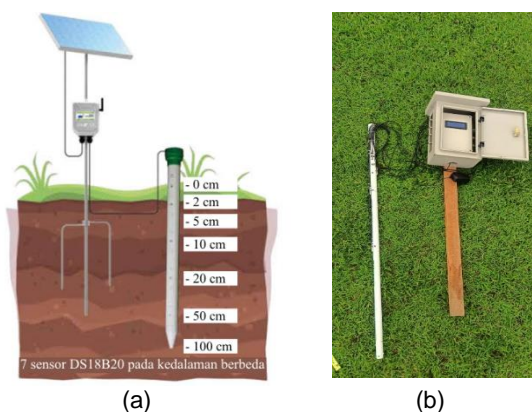


**Figure 5.** Concept (a) and realization (b) of the design of the digital soil temperature observation device used in the study

The written program reads data from the DS18B20 sensor and sends it to the server using the MQTT protocol. The RTC module is programmed to make

the sensor measure soil temperature every 10 seconds. There is a 20x4 LCD used to display the soil temperature measurement data. In addition, the ESP8266 module, connected to the internet via WiFi, is also programmed to send the soil temperature observation data every 10 seconds to the server for input into a database that can be accessed through the webpage <http://monitoringsuhutanah.my.id>.



**Figure 6.** Installation of the digital soil temperature observation equipment on October 17, 2023.

##### b) Software implementation

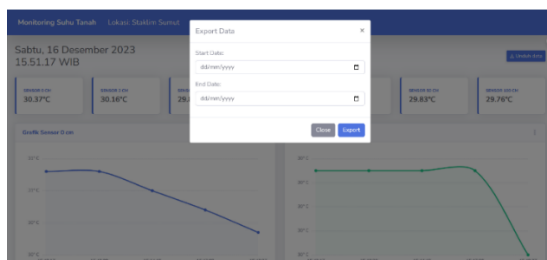


**Figure 7.** Real-time web display of soil temperature observations on the webpage: <http://monitoringsuhutanah.my.id/>

The software implementation in this study includes the development of a data display hosting on the webpage <http://monitoringsuhutanah.my.id>. This web hosting is utilized as a medium to display soil temperature data in real-time and store the data in the cloud. The data received by the server are then displayed in digital and graphical forms (using the last five readings), as shown in Figure 7. The data stored in the database can be exported into a Worksheet file (.xlsx) for specific date periods (Start- and End-date).

#### 3.2 Sensors Calibration

The calibration of the DS18B20 sensor used in this study was conducted at the Meteorological Equipment Calibration Laboratory of the Center for Meteorology, Climatology and Geophysics Region I (BBMKG Wilayah I Medan), on October 15, 2023, starting at 10:00 WIB until completion. Figure 8 is the documentation photos of the DS18B20 sensor calibration activity in this research. The sensor was placed alongside a standard sensor, followed by repeated measurements four times at each sample point. A data logger was placed adjacent to the standard temperature reading-display to facilitate recording the readings from each sensor.



**Figure 8.** The documentation photos of the DS18B20 sensor calibration at the Equipment Calibration Laboratory of the BBMKG Wilayah I Medan

**a) Calibration of the DS18B20 sensor depth 0 cm**

Table 2 presents the calibration results of the DS18B20 sensor at a depth of 0 cm. The calibration results indicate that the DS18B20 sensor at 0 cm depth has corrections at the set point of 15°C by -0.07, 25°C by -0.03, and 35°C by -0.08. The correction values for the DS18B20 sensor at 0 cm depth at each measurement set point are still within the tolerance value established by the World Meteorological Organization (WMO), which is  $\pm 0.2^\circ\text{C}$ . Based on these correction values, an adjustment of  $+0.04^\circ\text{C}$  is made to the DS18B20 sensor at a depth of 2 cm.

**b) Calibration of the DS18B20 sensor depth 2 cm**

Table 3 presents the calibration results of the DS18B20 sensor at a depth of 2 cm. The calibration results show that the DS18B20 sensor at 2 cm depth has corrections at the set point of 15°C by 0.29, 25°C by 0.33, and 35°C by 0.32. The correction values for the DS18B20 sensor at 2 cm depth at each measurement set point are slightly higher than the tolerance value established by the World Meteorological Organization (WMO), which is  $\pm 0.2^\circ\text{C}$ . Based on correction values, an adjustment of  $-0.24^\circ\text{C}$  is made to the DS18B20 sensor at a depth of 2 cm.

**c) Calibration of the DS18B20 sensor depth 5 cm**

Table 4 presents the calibration results of the DS18B20 sensor at a depth of 5 cm. The calibration results show that the DS18B20 sensor at 5 cm depth has corrections at the set point of 15°C by -0.21, 25°C by -0.30, and 35°C by -0.28. The correction values for the DS18B20 sensor at 5 cm depth at each measurement set point are slightly higher than the tolerance value established by the World Meteorological Organization (WMO), which is  $\pm 0.2^\circ\text{C}$ . Based on correction values, an adjustment of  $+0.20^\circ\text{C}$  is made to the DS18B20 sensor at a depth of 5 cm.

**Table 2.** Calibration data of the DS18B20 sensor depth 0 cm

Set Point	Standard Device ( $^\circ\text{C}$ )			DS18B20 Sensor depth 0 cm ( $^\circ\text{C}$ )		Average
	Measurement	Correction	Standard Temp	Measurement	Correction	
15°C	15.1336	0.0002	15.1338	15.21	-0.08	-0.07
	15.1334	0.0002	15.1336	15.23	-0.10	
	15.1340	0.0002	15.1342	15.19	-0.06	
	15.1344	0.0002	15.1346	15.20	-0.07	
25°C	25.0418	0.0120	25.0538	25.12	-0.07	-0.03
	25.0415	0.0120	25.0535	25.07	-0.02	
	25.0425	0.0120	25.0545	25.04	0.01	
	25.0410	0.0120	25.0530	25.09	-0.04	
35°C	35.0400	0.0200	35.0600	35.13	-0.07	-0.08
	35.0411	0.0200	35.0611	35.14	-0.08	
	35.0401	0.0200	35.0601	35.13	-0.07	
	35.0396	0.0200	35.0596	35.15	-0.09	
<b>Average Correction:</b>						<b>-0.04</b>

**d) Calibration of the DS18B20 sensor depth 10 cm**

Table 5 presents the calibration results of the DS18B20 sensor at a depth of 10 cm. The calibration results indicate that the DS18B20 sensor at 10 cm depth has corrections at the set point of 15°C by 0.25, 25°C by 0.27, and 35°C by 0.37. The correction values for the DS18B20 sensor at 10 cm depth at each measurement set point are slightly higher than the tolerance value established by the World Meteorological Organization (WMO), which is  $\pm 0.2^\circ\text{C}$ . Based on correction values, an adjustment of  $-0.23^\circ\text{C}$  is made to the DS18B20 sensor at a depth of 10 cm.

**e) Calibration of the DS18B20 sensor depth 20 cm**

Table 6 presents the calibration results of the DS18B20 sensor at a depth of 20 cm. The calibration results indicate that the DS18B20 sensor at 20 cm depth has corrections at the set point of 15°C by -0.19, 25°C by -0.20, and 35°C by -0.20. The correction values for the DS18B20 sensor at 20 cm depth at each measurement set point are slightly higher than the tolerance value established by the World Meteorological Organization (WMO), which is  $\pm 0.2^\circ\text{C}$ . Based on correction values, an adjustment of  $+0.15^\circ\text{C}$  is made to the DS18B20 sensor at a depth of 20 cm.

**f) Calibration of the DS18B20 sensor depth 50 cm**

Table 7 presents the calibration results of the DS18B20 sensor at a depth of 50 cm. The calibration results show that the DS18B20 sensor at 50 cm depth has corrections at the set point of 15°C by -0.16, 25°C by -0.18, and 35°C by -0.20. The correction values for the DS18B20 sensor at 50 cm depth at each measurement set point are slightly higher than the tolerance value established by the World Meteorological Organization (WMO), which is  $\pm 0.2^\circ\text{C}$ . Based on correction values, an adjustment of  $+0.13^\circ\text{C}$  is made to the DS18B20 sensor at a depth of 50 cm.

**g) Calibration of DS18B20 sensor depth 100 cm**

Table 8 presents the calibration results of the DS18B20 sensor at a depth of 100 cm. The calibration results indicate a correction at the set point of 15°C by -0.11, 25°C by -0.20, and 35°C by -0.16. The correction values are slightly higher than the tolerance value established by the World Meteorological Organization (WMO), which is  $\pm 0.2^\circ\text{C}$ . Based on correction values, an adjustment of  $+0.12^\circ\text{C}$  is made to the DS18B20 sensor at a depth of 100 cm.

**Table 3.** Calibration data of the DS18B20 sensor depth 2 cm

Set Point	Standard Device (°C)			DS18B20 Sensor depth 0 cm (°C)		Average
	Measurement	Correction	Standard Temp	Measurement	Correction	
15°C	15.1336	0.0002	15.1338	14.78	0.35	0.29
	15.1334	0.0002	15.1336	14.83	0.30	
	15.1340	0.0002	15.1342	14.85	0.28	
	15.1344	0.0002	15.1346	14.92	0.21	
25°C	25.0418	0.0120	25.0538	24.72	0.33	0.33
	25.0415	0.0120	25.0535	24.67	0.38	
	25.0425	0.0120	25.0545	24.8	0.25	
	25.0410	0.0120	25.0530	24.69	0.36	
35°C	35.0400	0.0200	35.0600	34.67	0.39	0.32
	35.0411	0.0200	35.0611	34.73	0.33	
	35.0401	0.0200	35.0601	34.83	0.23	
	35.0396	0.0200	35.0596	34.72	0.34	
<b>Average Correction:</b>						<b>0.24</b>

**Table 4.** Calibration data of the DS18B20 sensor depth 5 cm

Set Point	Standard Device (°C)			DS18B20 Sensor depth 0 cm (°C)		Average
	Measurement	Correction	Standard Temp	Measurement	Correction	
15°C	15.1336	0.0002	15.1338	15.38	-0.25	-0.21
	15.1334	0.0002	15.1336	15.33	-0.20	
	15.1340	0.0002	15.1342	15.25	-0.12	
	15.1344	0.0002	15.1346	15.42	-0.29	
25°C	25.0418	0.0120	25.0538	25.32	-0.27	-0.30
	25.0415	0.0120	25.0535	25.47	-0.42	
	25.0425	0.0120	25.0545	25.34	-0.29	
	25.0410	0.0120	25.0530	25.29	-0.24	
35°C	35.0400	0.0200	35.0600	35.37	-0.31	-0.28
	35.0411	0.0200	35.0611	35.23	-0.17	
	35.0401	0.0200	35.0601	35.33	-0.27	
	35.0396	0.0200	35.0596	35.42	-0.36	
<b>Average Correction:</b>						<b>-0.20</b>

**Table 5.** Calibration data of the DS18B20 sensor depth 10 cm

Set Point	Standard Device (°C)			DS18B20 Sensor depth 0 cm (°C)		Average
	Measurement	Correction	Standard Temp	Measurement	Correction	
15°C	15.1336	0.0002	15.1338	14.88	0.25	0.25
	15.1334	0.0002	15.1336	14.93	0.20	
	15.1340	0.0002	15.1342	14.79	0.34	
	15.1344	0.0002	15.1346	14.92	0.21	
25°C	25.0418	0.0120	25.0538	24.82	0.23	0.27
	25.0415	0.0120	25.0535	24.77	0.28	
	25.0425	0.0120	25.0545	24.74	0.31	
	25.0410	0.0120	25.0530	24.79	0.26	
35°C	35.0400	0.0200	35.0600	34.57	0.49	0.37
	35.0411	0.0200	35.0611	34.63	0.43	
	35.0401	0.0200	35.0601	34.83	0.23	
	35.0396	0.0200	35.0596	34.72	0.34	
<b>Average Correction:</b>						<b>0.23</b>

**Table 6.** Calibration data of the DS18B20 sensor depth 20 cm

Set Point	Standard Device (°C)			DS18B20 Sensor depth 0 cm (°C)		Average
	Measurement	Correction	Standard Temp	Measurement	Correction	
15°C	15.1336	0.0002	15.1338	15.28	-0.15	-0.19
	15.1334	0.0002	15.1336	15.33	-0.20	
	15.1340	0.0002	15.1342	15.25	-0.12	
	15.1344	0.0002	15.1346	15.42	-0.29	
25°C	25.0418	0.0120	25.0538	25.22	-0.17	-0.20
	25.0415	0.0120	25.0535	25.27	-0.22	
	25.0425	0.0120	25.0545	25.34	-0.29	
	25.0410	0.0120	25.0530	25.19	-0.14	
35°C	35.0400	0.0200	35.0600	35.27	-0.21	-0.20
	35.0411	0.0200	35.0611	35.23	-0.17	
	35.0401	0.0200	35.0601	35.33	-0.27	
	35.0396	0.0200	35.0596	35.22	-0.16	
<b>Average Correction:</b>						<b>-0.15</b>

Table 7. Calibration data of the DS18B20 sensor depth 50 cm

Set Point	Standard Device (°C)			DS18B20 Sensor depth 0 cm (°C)		Average
	Measurement	Correction	Standard Temp	Measurement	Correction	
15°C	15.1336	0.0002	15.1338	15.28	-0.15	-0.16
	15.1334	0.0002	15.1336	15.33	-0.20	
	15.1340	0.0002	15.1342	15.25	-0.12	
	15.1344	0.0002	15.1346	15.32	-0.19	
25°C	25.0418	0.0120	25.0538	25.22	-0.17	-0.18
	25.0415	0.0120	25.0535	25.27	-0.22	
	25.0425	0.0120	25.0545	25.24	-0.19	
	25.0410	0.0120	25.0530	25.19	-0.14	
35°C	35.0400	0.0200	35.0600	35.27	-0.21	-0.20
	35.0411	0.0200	35.0611	35.23	-0.17	
	35.0401	0.0200	35.0601	35.33	-0.27	
	35.0396	0.0200	35.0596	35.22	-0.16	
<b>Average Correction:</b>						<b>-0.13</b>

Table 8. Calibration data of the DS18B20 sensor depth 100 cm

Set Point	Standard Device (°C)			DS18B20 Sensor depth 0 cm (°C)		Average
	Measurement	Correction	Standard Temp	Measurement	Correction	
15°C	15.1336	0.0002	15.1338	15.18	-0.05	-0.11
	15.1334	0.0002	15.1336	15.33	-0.20	
	15.1340	0.0002	15.1342	15.25	-0.12	
	15.1344	0.0002	15.1346	15.22	-0.09	
25°C	25.0418	0.0120	25.0538	25.3	-0.25	-0.20
	25.0415	0.0120	25.0535	25.27	-0.22	
	25.0425	0.0120	25.0545	25.24	-0.19	
	25.0410	0.0120	25.0530	25.19	-0.14	
35°C	35.0400	0.0200	35.0600	35.17	-0.11	-0.16
	35.0411	0.0200	35.0611	35.23	-0.17	
	35.0401	0.0200	35.0601	35.23	-0.17	
	35.0396	0.0200	35.0596	35.27	-0.21	
<b>Average Correction:</b>						<b>-0.12</b>

### 3.3 Field Test

The field test was conducted by placing the digital soil temperature observation device near the conventional soil temperature observation equipment. The purpose of the field test was to compare the observations of soil temperature using the DS18B20 sensor in the digital device against the conventional device using a thermometer. In this study, the field test activities were carried out in the instrument garden of the North Sumatra Climatological Station (as shown in Figure 9) from October 18, 2023, at 07:00 LT until December 13, 2023, at 00:00 LT.

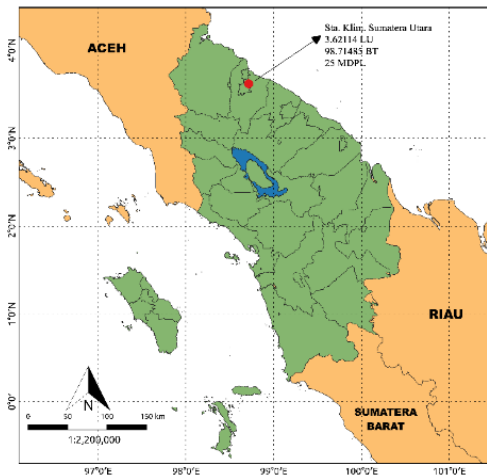


Figure 9. Location of field test in the Medan city.

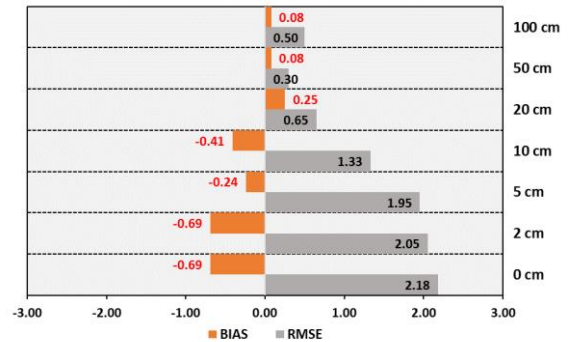


Figure 10. Graphic of bias and RMSE.

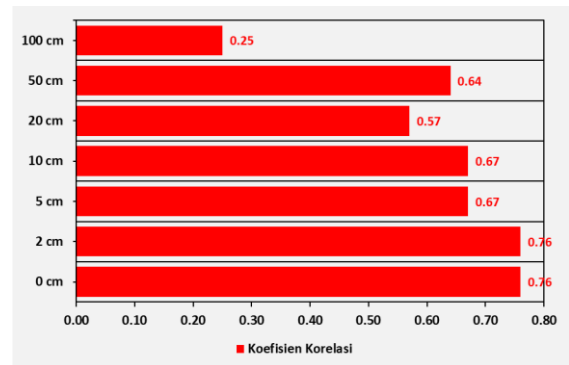
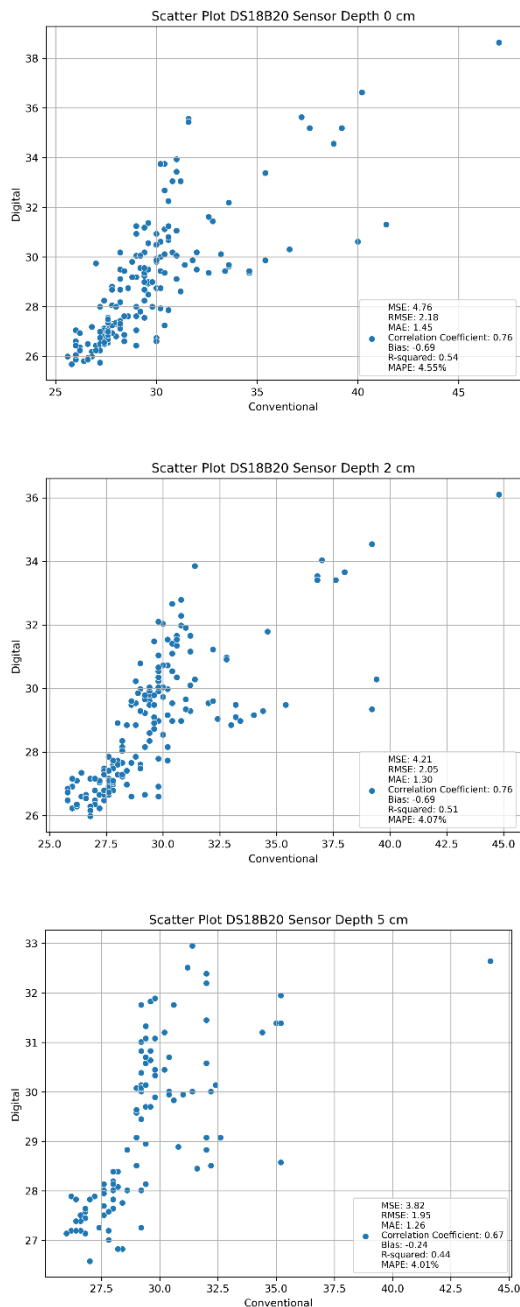
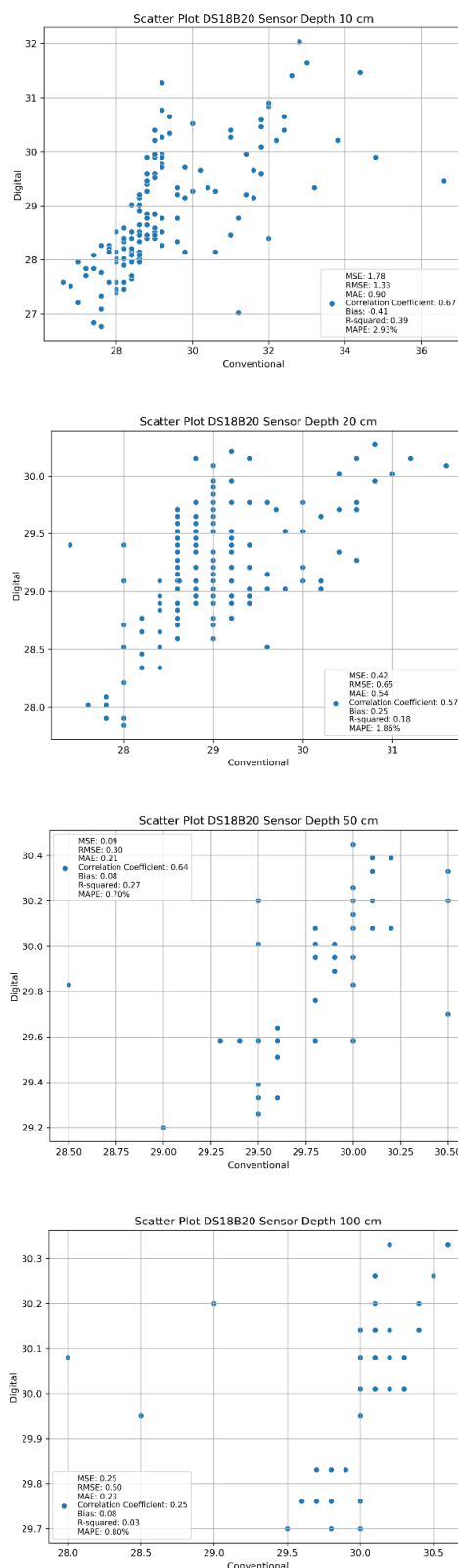


Figure 11. Graphic of correlation coefficient.

Figure 10 and Figure 11 show the values of bias, RMSE (Root Mean Square Error), and the correlation coefficient in comparing digital data against observational data during the field test. Figure 12 shows the scatter plots of digital and conventional data at each depth. An RMSE ranging from 0.5 to 2.18 indicates that the digital data are considered quite accurate and provide results consistent with the conventional method. A negative bias value at depths of 0 cm, 2 cm, 5 cm, and 10 cm implies that the sensor tends to measure soil temperature lower than the conventional device.



indicate a positive (linear) relationship between the digital and conventional data.



Conversely, a positive bias at depths of 20 cm, 50 cm, and 100 cm suggests that the sensor tends to measure higher soil temperatures compared to the conventional device. Generally, a bias value close to zero indicates a small difference between the digital and conventional data. The correlation coefficient values ranging from 0.25 to 0.76

Figure 12. Scatter plot of digital and conventional data distribution at various depths

It is observed that the deeper the sensor is placed, the smaller the correlation coefficient, indicating a weaker agreement between the sensor

and conventional measurements. Based on the field test results, it is observed that at shallower depths, the digital sensor tends to provide more consistent results with the conventional method. As depth increases, the correlation between digital sensor readings and conventional readings weakens, which may be due to environmental factors affecting sensor such as temperature, humidity, or soil composition.

## 6. Conclusion

The use of the DS18B20 sensor and ESP8266 module in the Internet of Things-based digital soil temperature observation system provides a real-time soil temperature monitoring tool with high temporal resolution. Calibration results confirm that soil temperature measurements by the DS18B20 sensor are accurate and consistent, making it suitable for operational use. The ESP8266 module enables easy access and readability of digital observation data over the internet. Field test results show that the digital sensor provides sufficiently accurate results, aligning well with the conventional device. Statistical measurements of accuracy reveal that the correlation values reach 0.6-0.7 (except for a depth of 100 cm, which is 0.25), while RMSE values range from 0.5 to 2.18 and bias ranges from (-0.69) to 0.08.

## 7. Recommendation

Further research should be conducted to develop the results of this study. This includes adding other weather parameter sensors, such as humidity, soil salinity, pH, and others, to provide a comprehensive analysis of soil conditions. The soil temperature profile at the North Sumatra Climatological Station can serve as supporting information for agricultural planning, such as selecting types of crops or determining irrigation timing.

## References

- ARDUINO corp. (2022). Arduino Integrated Development Environment (IDE) v1 | Arduino Documentation | Arduino Documentation. on *Arduino Docs*.
- Asnawi, Y., Simanjuntak, A. V., Umar, M., Rizal, S., & Syukri, M. (2020). A Microtremor Survey to Identify Seismic Vulnerability Around Banda Aceh Using HVSR Analisis. *Elkawanie: Journal of Islamic Science and Technology*, 6(2), 342-358.
- Asnawi, Y., Simanjuntak, A., Muksin, U., Rizal, S., Syukri, M. S. M., Maisura, M., & Rahmati, R. (2022). Analysis of microtremor H/V spectral ratio and public perception for disaster mitigation. *GEOMATE Journal*, 23(97), 123-130.
- Atzori, L., Iera, A., & Morabito, G. (2010). The Internet of Things: A survey. *Computer Networks*, 54(15), 2787-2805. <https://doi.org/10.1016/j.comnet.2010.05.010>
- Brady, N. C., Weil, R. R., & Weil, R. R. (2008). *The nature and properties of soils* (Vol. 13). Prentice Hall Upper Saddle River, NJ.
- Campbell, G. S., & Norman, J. M. (1998). *An Introduction to Environmental Biophysics* (2nd Edition). Springer Science & Business Media.
- Dallas Semiconductor. (2002). DS18B20 Temperature Sensor. *Dallas semiconductor datasheets*.
- Espressif Systems. (2023). *ESP8266EX Datasheet* (7.0). Espressif Systems.
- Hatfield, J. L., & Prueger, J. H. (2015). Temperature extremes: Effect on plant growth and development. *Weather and Climate Extremes*, 10. <https://doi.org/10.1016/j.wace.2015.08.001>
- Idha, R., Sari, E. P., Asnawi, Y., Simanjuntak, A. V., Humaidi, S., & Muksin, U. (2023). 1-Dimensional Model of Seismic Velocity after Tarutung Earthquake 1 October 2022 Mw 5.8. *Journal of Applied Geospatial Information*, 7(1), 825-831.
- Maxim Integrated. (2015). DS18B20 Programmable Resolution 1-Wire Digital Thermometer General Description. *Datasheet*, 92.
- Muksin, U., Arifullah, A., Simanjuntak, A. V., Asra, N., Muzli, M., Wei, S., ... & Okubo, M. (2023). Secondary fault system in Northern Sumatra, evidenced by recent seismicity and geomorphic structure. *Journal of Asian Earth Sciences*, 245, 105557.
- Nurana, I., Simanjuntak, A. V. H., Umar, M., Kuncoro, D. C., Syamsidik, S., & Asnawi, Y. (2021). Spatial Temporal Condition of Recent Seismicity in The Northern Part of Sumatra. *Elkawanie: Journal of Islamic Science and Technology*, 7(1), 131-145.
- Preston-Thomas, H. (1990). The International Temperature Scale of 1990(ITS-90). *Metrologia*, 27(1), 3-10.
- Rose, C. W. (2004). *An Introduction to the Environmental Physics of Soil, Water and Watersheds*. Cambridge University Press.
- Salam, A. K. (2020). *Ilmu Tanah*. Global Madani Press.
- Saragih, I. J. A., Kristianto, A., Silitonga, A. K., & Paski, J. A. I. (2017). Kajian Dinamika Atmosfer saat Kejadian Hujan Lebat di Wilayah Pesisir Timur Sumatera Utara Menggunakan Model WRF-ARW dan Citra Satelit Himawari-8. *Unnes Physics Journal*, 6(1), 25-30.
- Saragih, I. J. A., Rumahorbo, I., Yudistira, R., & Suchayono, D. (2020). Prediksi Curah Hujan Bulanan Di Deli Serdang Menggunakan Persamaan Regresi Dengan Prediktor Data Suhu Dan Kelembapan Udara. *Jurnal Meteorologi Klimatologi dan Geofisika*, 7(2), 6-14.
- Saragih, I. J. A., Mukhsinin, H. A., Tarigan, K., Sinambela, M., Situmorang, M., Sembiring, K., & Humaidi, S. (2021, November). Improvement in WRF model prediction for heavy rain events over North Sumatra region using satellite data assimilation. In *IOP Conference Series: Earth and Environmental Science* (Vol. 893, No. 1, p. 012040). IOP Publishing.
- Sari, E. P., Idha, R., Asnawi, Y., Simanjuntak, A., Humaidi, S., & Muksin, U. (2023). Faulting Mechanism of Tarutung Earthquake 2022 Mw 5.8 Using Moment Tensor

- Inversion. *Journal of Applied Geospatial Information*, 7(1), 840-846.
- Simanjuntak, A. V., & Ansari, K. (2022). Seismicity clustering of sequence phenomena in the active tectonic system of backthrust Lombok preceding the sequence 2018 earthquakes. *Arabian Journal of Geosciences*, 15(23), 1730.
- Simanjuntak, A. V., & Ansari, K. (2023). Spatial time cluster analysis and earthquake mechanism for unknown active fault (Kalatoa fault) in the Flores Sea. *Earth Science Informatics*, 16(3), 2649-2659.
- Simanjuntak, A. V., Muksin, U., & Setiawan, Y. (2019, June). Source Mechanism Analysis By Using Tensor Moment Inversion (Study Case: Pidie Jaya Earthquake in 2016 December 7th). In *IOP Conference Series: Earth and Environmental Science* (Vol. 273, No. 1, p. 012021). IOP Publishing.
- Simanjuntak, A. V., Muksin, U., & Sipayung, R. M. (2018, December). Earthquake relocation using HypoDDMethod to investigate active fault system in Southeast Aceh. In *Journal of Physics: Conference Series* (Vol. 1116, No. 3, p. 032033). IOP Publishing.
- Simanjuntak, A. V., Palgunadi, K. H., Supendi, P., Daryono, D., Prakoso, T. A., & Muksin, U. (2023). New Insight on the Active Fault System in the Halmahera Volcanic Arc, Indonesia, Derived from the 2022 Tobelo Earthquakes. *Seismological Research Letters*, 94(6), 2586-2594.
- Simanjuntak, A., Muksin, U., Asnawi, Y., Rizal, S., & Wei, S. (2022). Recent Seismicity and Slab Gap Beneath Toba Caldera (Sumatra) Revealed Using Hypocenter Relocation Methodology. *Geomate Journal*, 23(99), 82-89.